Set-Based Line-of-Sight (LOS) Path Following with Collision Avoidance for Underactuated Unmanned Surface Vessel

Signe Moe[1] and Kristin Y. Pettersen[1]

Abstract— A cornerstone ability of an autonomous unmanned surface vessel (USV) is to avoid collisions with stationary obstacles and other moving vehicles while following a predefined path. USVs are typically underactuated, and this paper extends recent results in set-based guidance theory to an underactuated surface vessel, resulting in a switched guidance system with a path following mode and a collision avoidance mode. This system can be used with any combination of path following and collision avoidance guidance laws. Furthermore, a specific guidance law for collision avoidance is suggested that ensures tracking of a safe radius about a moving obstacle. The guidance law is specifically designed to assure collision avoidance while abiding by the International Regulations for Preventing Collisions at Sea (COLREGs). It is proven that the USV successfully circumvents the obstacles in a COLREGs compliant manner and that path following is achieved in path following mode. Simulations results confirm the effectiveness of the proposed approach.

I. INTRODUCTION

To plan and control the motion of a marine vessel, a guidance, navigation and control (GNC) system is required [1]. Typically, surface vessels generally only have actuators in surge (thruster force) and yaw (rudder angle or azimuth thrusters), while they do not have any actuators in the sideways direction (sway). This underactuation must be taken into account in the guidance and control system. Typically, for an USV with a path following task, the guidance system consists of guidance laws for heading and surge velocity that, if satisfied, ensure convergence to the desired path. The control system calculates the thruster force and rudder angle to track the reference states delivered by the guidance system. This paper considers a guidance and control system that enables an underactuated USV to avoid moving obstacles while following a given path.

A commonly used approach for path following is the Line of Sight (LOS) method, which allows for following of straight line paths [2], [3] and curved paths [4]-[5]. This approach can be expanded to counteract environmental disturbances and thereby achieve path following also in the presence of ocean currents [6], [7]. Another possible approach is using backstepping techniques to ensure path following [8]-[10]. However, these pure path following algorithms aim at following a predefined path and do not consider collision avoidance.

In nautical navigation, all surface vessels are subject to COLREGs [11]. A variety of approaches have been proposed for collision avoidance, both for the general and maritime case, such as potential fields [12], dynamic window [13], [14] and velocity obstacles [11], [15]. However, these approaches have several drawbacks. Potential fields may suffer from oscillating behavior and other limitations [16]. The dynamic window approach assumes no sideways velocity, and is therefore not suitable for USVs since these are able to and will glide sideways while moving through water. Furthermore, the dynamic window approach can be computationally heavy. However, it can easily be modified to comply with COLREGs [14]. Finally, the velocity obstacle (VO) approach has good mathematical qualities, is computationally simple and does easily comply with COLREGs. However, it assumes linear velocities, is not straight-forward to implement and it is not obvious how to combine VO with existing guidance methods.

In this paper, we will present a guidance and control system that takes into account the underactuation of the USV. The system guarantees collision avoidance of moving and static obstacles while ensuring path following of a predefined desired path. To achieve this, we utilize recent results that makes it possible to incorporate set-based tasks into a well-known prioritized task guidance framework. This method is presented for a general robotic system in [17], [18] and is experimentally validated in [19]. Set-based tasks are relevant for the collision avoidance problem because a set-based task has a valid interval of values rather than an exact desired value, and collision avoidance may thus be considered as a set-based task defined as the distance between the USV and obstacle where the valid interval of the task has a lower bound of some minimum safe distance. The method presented in [17], [18] is, however, developed for fully actuated and redundant systems, and thus it cannot be directly applied to an underactuated surface vessel.

The contribution of this paper is twofold. Firstly, this paper suggests using set-based theory to satisfy two objectives: Collision avoidance and path following. The approach is adapted to the underactuated USV by switching between two predefined guidance laws rather than combining them using the Null-Space-Based Inverse Kinematics approach for fully actuated systems as in [17], [18]. The guidance laws, if satisfied, will ensure path following and collision avoidance respectively. Thus the system is equipped with one path following mode and one collision avoidance mode, in addition to a defined and deterministic method for switching between these two. This results in a tighter coupling between

[1]S.Moe and K.Y.Pettersen are with the Center for Autonomous Marine Operations and Systems (AMOS), at The Department of Engineering Cybernetics, Norwegian University of Science and Technology (NTNU), Trondheim, Norway {signe.moe, kristin.y.pettersen}@itk.ntnu.no

collision avoidance, path planning and guidance than standard VO implementations. Furthermore, this method can be used for any combination of path following and collision avoidance guidance laws, making it a highly generic solution. Secondly, a specific LOS-based guidance law for collision avoidance is suggested. This guidance law, if satisfied, will ensure that the USV tracks a circle with constant radius about the obstacle center, which may be stationary or moving, and is specifically designed to assure collision avoidance while abiding by the COLREGs.

A similar approach is presented in [20] where the system smoothly switches between a path following task and an collision avoidance task. However, only stationary obstacles are considered. Furthermore, the switching between path following and collision avoidance in [20] is given as a smooth transition function dependent on the distance between the USV and the obstacle center, which results in a potential field approach with known drawbacks as discussed above. This problem is avoided in this paper by using set-based theory as a switching criterion rather than a smoothing function. Furthermore, we consider also moving obstacles.

This paper is organized as follows: The vessel model and the control objective are given in Section II and III, respectively. The suggested guidance and control system is presented in Section IV and the main results in Section V before simulation results are given in Section VI. Conclusions in Section VII.

II. VESSEL MODEL

This section presents the 3-DOF surface USV maneuvering model that is considered and the assumptions on which this is based.

A. Model Assumptions

Assumption 1. The motion of the USV is described by 3 degrees of freedom (DOF), that is surge, sway and yaw.

Assumption 2. The USV is port-starboard symmetric.

Assumption 3. The body-fixed coordinate frame b is located in a point $(x_g^\star, 0)$ from the USV's center of gravity (CG) along the center-line of the ship.

Remark 1. The body-fixed coordinate system can always be translated to the required location $x_g^\star$ [1].

Assumption 4. The hydrodynamic damping is linear.

Remark 2. The passive nature of the nonlinear hydrodynamic damping forces should enhance the directional stability of the USV.

B. The Vessel Model

The state of the USV is given by the vector $\boldsymbol{\eta} \triangleq [x, y, \psi]^T$ and describes the position (x, y) and the orientation ψ of the USV with respect to the inertial frame i. The vector $\boldsymbol{v} \triangleq [u, v, r]^T$ contains the linear and angular velocities of the USV defined in the body-fixed frame b, where u is the surge velocity, v is the sway velocity and r is the yaw rate. The body frame is rotated with respect to the inertial frame through the rotation matrix

$$\boldsymbol{R}(\psi) \triangleq \begin{bmatrix} \cos(\psi) & -\sin(\psi) & 0 \\ \sin(\psi) & \cos(\psi) & 0 \\ 0 & 0 & 1 \end{bmatrix}. \quad (1)$$

The following 3-DOF maneuvering model is considered [1], [6]:

$$\begin{aligned} \dot{\boldsymbol{\eta}} &= \boldsymbol{R}(\psi)\boldsymbol{v} \\ \boldsymbol{M}\dot{\boldsymbol{v}} + \boldsymbol{C}(\boldsymbol{v})\boldsymbol{v} + \boldsymbol{D}\boldsymbol{v} &= \boldsymbol{B}\boldsymbol{f} \end{aligned} \quad (2)$$

The vector $\boldsymbol{f} \triangleq [T, \delta]^T$ contains the control inputs: T is the thruster force and δ is the rudder angle. The mass and inertia matrix $\boldsymbol{M}$ is symmetric and positive definite and includes hydrodynamic added mass, $\boldsymbol{C}$ is the Coriolis and centripetal matrix and $\boldsymbol{D}$ is the positive definite hydrodynamic damping matrix. $\boldsymbol{B} \in \mathbb{R}^{3 \times 2}$ is the actuator configuration matrix. The matrices have the following structure:

$$\boldsymbol{M} \triangleq \begin{bmatrix} m_{11} & 0 & 0 \\ 0 & m_{22} & m_{23} \\ 0 & m_{23} & m_{33} \end{bmatrix}, \boldsymbol{D} \triangleq \begin{bmatrix} d_{11} & 0 & 0 \\ 0 & d_{22} & d_{23} \\ 0 & d_{32} & d_{33} \end{bmatrix}, \boldsymbol{B} \triangleq \begin{bmatrix} b_{11} & 0 \\ 0 & b_{22} \\ 0 & b_{32} \end{bmatrix}$$

$$\boldsymbol{C}(\boldsymbol{v}) \triangleq \begin{bmatrix} 0 & 0 & -m_{22}v - m_{23}r \\ 0 & 0 & m_{11}u \\ m_{22}v + m_{23}r & -m_{11}u & 0 \end{bmatrix}$$

$$(3)$$

Assumptions 1-4 justify the structure of $\boldsymbol{M}$ and $\boldsymbol{D}$ and the structure of $\boldsymbol{C}$ is obtained as described in [1]. Furthermore, the point $x_g^\star$ from Assumption 3 is chosen so that $\boldsymbol{M}^{-1}\boldsymbol{B}\boldsymbol{f} = [\tau_u, 0, \tau_r]^T$. This point $(x_g^\star, 0)$ exists for all port-starboard symmetric ships [21].

Remark 3. It is shown in [1] that the ship can be described by the 3-DOF maneuvering model in (2).

C. The Model in Component Form

For the control design is it useful to expand (2) into component form:

$$\begin{aligned} \dot{x} &= \cos(\psi)u - \sin(\psi)v, \\ \dot{y} &= \sin(\psi)u + \cos(\psi)v, \\ \dot{\psi} &= r, \\ \dot{u} &= F_u(v, t) - \frac{d_{11}}{m_{11}}u + \tau_u, \\ \dot{v} &= X(u)r + Y(u)v, \\ \dot{r} &= F(u, v, r) + \tau_r \end{aligned} \quad (4)$$

The expressions for F_u, $X(u)$, $Y(u)$ and $F(u, v, r)$ are given in the Appendix A.

III. CONTROL OBJECTIVES

This section formalizes the control problem solved in this paper. The USV has several objectives: avoid all obstacles in a COLREGs compliant manner, follow a predefined path C and keep a given surge velocity along the path. It is clear that the two first objectives may be in conflict. Hence, in the case both cannot be achieved, collision avoidance needs to have first priority to ensure safe passage of the USV.

The path cross-track error y_e is computed as the shortest distance between the USV and any point on the path, and is defined so that $y_e = 0$ implies that the USV is on the desired path. In the case of a path parametrized as a function of θ it is the orthogonal distance between the USV position (x, y) to the path-tangential reference frame defined by the point

$(x_p(\theta), y_p(\theta))$. It is assumed that the path is an open curve, i.e. the end point is different from the start point.

The control objectives are formalized in prioritized order below:

1) The distance between the USV and every obstacle with position $\boldsymbol{p}_o(t)$ should always be greater than or equal to some safe distance R_o:
$$|\boldsymbol{p}(t) - \boldsymbol{p}_o(t)| \geq R_o \quad \forall \ t \geq t_0 \qquad (5)$$

2) The USV position should converge to the desired path.
$$\lim_{t \to \infty} y_e(t) = 0 \qquad (6)$$

3) The USV surge velocity should track to some desired, positive velocity.
$$\lim_{t \to \infty} u(t) = u_{\text{des}}(t) \qquad (7)$$

Note that $u_{\text{des}}(t)$ will be provided by the set-based guidance system and will depend on the mode of the system, i.e. if the USV is in path following mode or collision avoidance mode.

IV. THE GUIDANCE AND CONTROL SYSTEM

This section presents the guidance and control system consisting of guidance laws and controllers. The guidance system consists of separate guidance laws for path following and collision avoidance, and an algorithm to switch between these two.

A. Guidance Laws for Path Following

The desired surge velocity u_{des} for path following is constant, positive and is denoted u_{pf}. Furthermore, the desired heading for path following is denoted ψ_{pf}, where ψ_{pf} is a suitable guidance law for following the desired path in question. For instance, in the case of a straight line path, a suitable choice for ψ_{pf} would be a LOS guidance law designed for straight paths as given in [22], which is proven to give UGAS and ULES, and thus makes the path cross-track error converge to zero.

Assumption 5. The path following guidance law is chosen so that, if fulfilled, the path cross-track error will converge to zero.

B. Guidance Laws for collision avoidance

This paper suggests a specific guidance law to safely avoid obstacles while abiding COLREGs. Note that this guidance law is completely independent of the set-based algorithm presented in the next subsection, and that it may be replaced by any other guidance law to ensure collision avoidance.

In the case of collision avoidance, the goal is to track a safe radius around the object center. If this radius is maintained, a collision will never occur. Denote the obstacle safe radius as R_o, the obstacle center as
$$\boldsymbol{p}_o(t) = \begin{bmatrix} x_c(t) & y_c(t) \end{bmatrix}^T \qquad (8)$$
and the obstacle velocity as
$$U_o = \sqrt{\dot{x}_c^2 + \dot{y}_c^2}. \qquad (9)$$

Assumption 6. The obstacle speed is upper bounded by $U_{o,\text{max}}$:
$$U_o \leq U_{o,\text{max}} \qquad (10)$$

Furthermore, denote
$$\phi = \arctan\left(\frac{y - y_c}{x - x_c}\right), \qquad (11)$$
$$\beta_o = \arctan\left(\frac{\dot{y}_c}{\dot{x}_c}\right), \qquad (12)$$
$$V_o = U_o \cos(\phi - \beta_o), \qquad (13)$$
where ϕ and β_o are illustrated in Fig. 1. The velocity V_o describes the velocity of the obstacle relative to the position of the USV, where a positive V_o suggests that the obstacle is moving closer to the USV. It reaches its maximum value of U_o when the obstacle is moving straight towards the current position of the USV (not taking the USV velocity or heading into account).

The desired surge velocity u_{des} for collision avoidance is constant, positive and is denoted u_{oa}.

Assumption 7. We assume that the obstacle speed is lower than the desired surge velocity, i.e.
$$u_{oa} > U_{o,\text{max}}. \qquad (14)$$

Remark 5. It is natural to assume that the USV moves sufficiently fast to avoid the obstacle by moving around it. Furthermore, Assumption 6 and 7 ensure that the term k in the collision avoidance heading guidance law (15) is real.

The following guidance law giving the desired heading for collision avoidance is proposed:
$$\psi_{oa} = \phi + \lambda \left(\frac{\pi}{2} - \arctan\left(\frac{e+k}{\Delta}\right)\right) - \arctan\left(\frac{v}{u_{oa}}\right), \qquad (15)$$
where $\lambda = 1$ corresponds to clock-wise motion and $\lambda = -1$ to counter-clockwise motion. Note that λ should be chosen in accordance with COLREGs, see Section IV-C. The guidance parameter $\Delta > 0$ is a design parameter corresponding to the look-ahead distance and e is the cross-track error of the circular path defined as
$$e = R_o - \rho = R_o - \sqrt{(x - x_c)^2 + (y - y_c)^2}, \qquad (16)$$
and k is defined as
$$k = \begin{cases} k_1 & V_o \geq 0 \\ k_2 & V_o < 0, \end{cases} \qquad (17)$$
$$k_{\{1,2\}} = \frac{-b\{+,-\}\sqrt{b^2 - 4ac}}{2a} \qquad (18)$$
$$\qquad (19)$$
where
$$a = U_{oa}^2 - V_o^2 = u_{oa}^2 + v^2 - V_o^2, \qquad (20)$$
$$b = -2V_o^2 e, \qquad (21)$$
$$c = -V_o^2(\Delta^2 + e^2). \qquad (22)$$
By Assumptions 6 and 7, it is easy to verify that $a > 0$ and $c \geq 0$. Hence $k_1 \geq 0$ and $k_2 \leq 0$. The parameter k is designed to compensate for the movement of the obstacle, and thus the sign of the compensation shifts as the USV traverses the obstacle radius and the movement of the obstacle relative to the USV changes.

Theorem 1. *Given Assumption 6 and 7, if the guidance laws $u_{\text{des}} = u_{oa}$ and $\psi_{\text{des}} = \psi_{oa}$ are satisfied, the cross-track error e will asymptotically converge to zero and the USV (4) will track the radius R_o about the obstacle center $\boldsymbol{p}_o(t)$.*
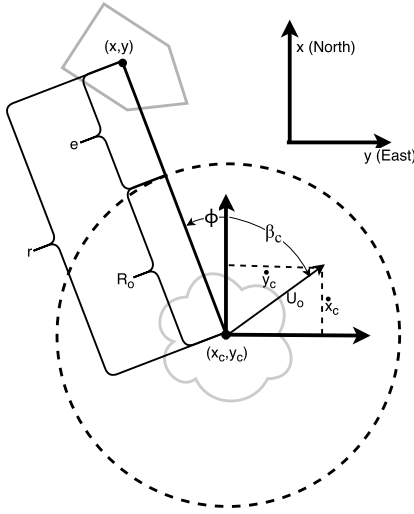
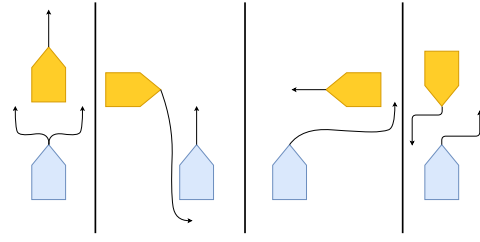Fig. 1: Illustration of parameters used for collision avoidance.

Fig. 2: COLREGs scenarioes and the correct behavior of the involved vessels. USV in shown in blue and obstacle in orange. From left to right: Overtaking, crossing from left, crossing from right, head-on.
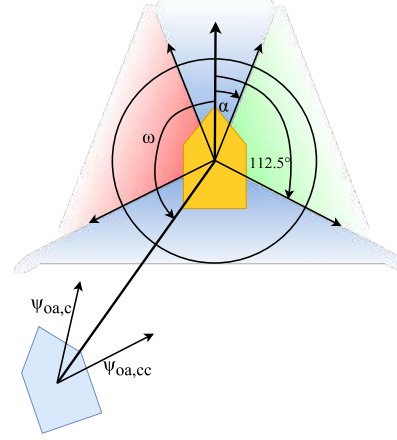

Fig. 3: The different COLREGs scenarios as function of ω. From the top and clockwise: Head-on, crossing from left, overtaking, crossing from right. This specific illustration displays an overtaking situation, which is the only scenario where the required direction of the motion (clockwise or counterclockwise) is not strictly specified by COLREGs. Therefore, the motion most aligned with the current heading is chosen, in this case clockwise, given by $\psi_{\mathrm{oa,c}}$.

Proof. See Appendix B. □

C. Choosing λ

In the guidance law for collision avoidance, λ determines whether the USV circumvents an obstacle with a clockwise or counterclockwise motion. COLREGs provides definitions and rules to the various collision avoidance scenarios, see Fig. 2 [11]. A formal classification is illustrated in Fig. 3.

- Overtaking: Overtaking is allowed on either side of the obstacle as long as the USV keeps a sufficient distance to the obstacle. COLREGs defines overtaking as approaching another vessel at more than 22.5 degrees abaft her beam. This corresponds to the angle ω (illustrated in Fig. 3) between the heading of the obstacle and the position of the USV is larger than $112.5°$ or less than $-112.5°$. This paper suggests considering both clockwise and counter-clockwise motion by calculating ψ_{oa} (15) for both $\lambda = -1$ (counterclockwise) and $\lambda = 1$ (clockwise), and denoting this as $\psi_{\mathrm{oa,cc}}$ and $\psi_{\mathrm{oa,c}}$ respectively. The direction closest to the current heading ψ of the USV is then chosen, thereby avoiding a sharp turn. This is formalized as

$$\lambda = \begin{cases} -1 & |\psi - \psi_{\mathrm{oa,cc}}| \leq |\psi - \psi_{\mathrm{oa,c}}| \\ 1 & |\psi - \psi_{\mathrm{oa,cc}}| > |\psi - \psi_{\mathrm{oa,c}}| \end{cases}. \quad (23)$$

- Crossing from left: In this case, the USV has the right of way. Technically, no collision avoidance should be activated. However, an autonomous system should be able to avoid a collision even in the case that the other vehicle does not abide by the rules. Hence, this paper suggests activating collision avoidance with $\lambda = -1$, corresponding to counterclockwise motion. Thus, if the obstacle complies with COLREGs, the USV's deviation of the path is minimized. Unlike overtaking, COLREGs does not specify a specific angle for this premise. Thus, this paper defines this scenario as $\omega \in [\alpha, 112.5°)$ for some positive angle α. In all simulations, $\alpha = 15°$ [23].

- Crossing from right: In this situation, the USV is the give-way vessel and must avoid the obstacle by moving

in a counterclockwise motion, indicating $\lambda = -1$. This scenario is defined as $\omega \in [-112.5°, -\alpha)$.

- Head-on: When two vessels meet head-on, both vehicles should alter course so that they will pass with the other vessel on their port side. This corresponds to a counterclockwise motion, therefore $\lambda = -1$. This case is activated when $\omega \in [-\alpha, \alpha)$.

Note that as the USV circumvents the obstacle and ω changes, the setting is not reclassified. Hence, as the set-based algorithm enters collision avoidance mode, it is determined what collision avoidance scenario is applicable and λ is determined as described above. This value for λ is kept until the next time the system enters obstacle mode.

D. Set-Based Guidance

The two previous subsections have presented guidance laws for surge velocity and heading for path following and collision avoidance. These two different scenarios are considered the two modes of the system, and we will in the following, based on the set-based control approach [18],

develop a method for switching between these two. Note that this approach can be used with any combination of methods for path following and collision avoidance and is not limited to the collision avoidance approach presented in the previous subsection.

We define the task σ as the distance between an obstacle center and the USV, which is given by ρ in (16):

$$\sigma = \rho = \sqrt{(x-x_c)^2 + (y-y_c)^2} \tag{24}$$

Rewriting into polar coordinates,

$$x - x_c = \rho \cos(\phi) \tag{25}$$

$$y - y_c = \rho \sin(\phi), \tag{26}$$

where ϕ is defined in (11), the task derivative is given as

$$
\begin{aligned}
\dot{\sigma} &= \frac{2(x-x_c)(\dot{x}-\dot{x}_c) + 2(y-y_c)(\dot{y}-\dot{y}_c)}{2\sqrt{(x-x_c)^2 + (y-y_c)^2}} \\
&= \frac{\rho \cos(\phi)(\dot{x}-\dot{x}_c) + \rho \sin(\phi)(\dot{y}-\dot{y}_c)}{\rho} \\
&= u\cos(\phi-\psi) + v\sin(\phi-\psi) - \sqrt{\dot{x}_c^2 + \dot{y}_c^2}\cos\left(\phi - \arctan\left(\frac{\dot{y}_c}{\dot{x}_c}\right)\right) \\
&= U\cos(\phi-\psi-\beta) - V_o. \tag{27}
\end{aligned}
$$

Furthermore, we define a mode change radius $R_m > R_o$ around the obstacle:

Assumption 8. The radius R_m is chosen sufficiently large that in case of a switch to collision avoidance modus, the USV can converge to the radius R_o without overshoot. This will depend on the velocities of the USV and obstacle, the look-ahead distance Δ and the maximum turning radius of the USV.

Given our specified control objectives (5)-(6), the desired behavior of the USV is to follow the desired path C as long as this is possible while avoiding collisions. Path following is therefore considered the default mode. If the USV is outside the radius R_m, path following is always active. However, in agreement with the method in [18], we allow the path following mode to be active inside R_m under the condition that this will increase or maintain the current distance between the obstacle center and the USV, i.e. if $\dot{\sigma} \geq 0$ with $u = u_{pf}$ and $\psi = \psi_{pf}$. In other words, inside R_m collision avoidance is active as long as the desired behavior in path following mode will result in the USV decreasing the distance to the obstacle. In this case, the guidance laws for collision avoidance will ensure that the USV converges to the safe distance R_o from the obstacle center until such a time that the path following guidance law will take the USV further away from the obstacle. This switching behavior can be captured by the *tangent cone*. The tangent cone to the set $D = [\sigma_{min}, \sigma_{max}]$ at the point $\sigma \in D$ is defined as

$$T_D(\sigma) = \begin{cases} [0, \infty) & \sigma = \sigma_{min} \\ \mathbb{R} & \sigma \in (\sigma_{min}, \sigma_{max}) \\ (-\infty, 0] & \sigma = \sigma_{max} \end{cases} \tag{28}$$

Note that $\dot{\sigma}(t) \in T_D(\sigma(t))$ $\forall$ $t \geq t_0$ implies that $\sigma(t) \in D$ $\forall t \geq t_0$. Thus, we can define a valid set D for our collision avoidance task and remain in path following mode as long as our collision avoidance task σ and the corresponding $\dot{\sigma}$ is in the tangent cone of D. We suggest defining

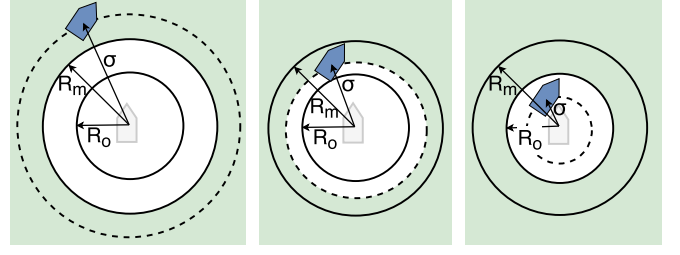$$D = [\min(R_m, \max(\sigma, R_o)), \infty), \tag{29}$$

Fig. 4: The set $D = [\min(R_m, \max(\sigma, R_o)), \infty)$ used in Algorithm 1 illustrated in green. Outside R_m (left), the USV is always in the tangent cone of D and thus path following mode is active. For $R_o \leq \sigma \leq R_m$ (center), σ is always on the lower border of D by definition. Hence, path following is active only if the corresponding $\dot{\sigma} \geq 0$. For $\sigma < R_o$ (right), the USV is outside the set D and the collision avoidance control objective is violated.

which is illustrated in Fig. 4. As long as $\sigma \in D$, the collision avoidance objective (5) is satisfied. A practical implementation of the tangent cone is given in Algorithm 2.

Thus, we define our control algorithm as in Algorithm 1 where in_T_C is the tangent cone function defined in Algorithm 2 and σ and $\dot{\sigma}$ are defined in (24) and (27) with $u = u_{pf}$ and $\psi = \psi_{pf}$. Note that in case of multiple obstacles, one has to consider one task per obstacle and check which obstacle, if any, is not in the tangent cone and thereby requires circumvention. The problem of overlapping obstacles is a topic for future work.

---

1 Initialize:
2 last_mode = path_following;
3 $\lambda = -1$;
4 **while** *True* **do**
5   a = in_T_C(σ, $\dot{\sigma}$, min(R_m, max(σ, R_o)), ∞);
6   **if** *a is True* **then**
7          $u_{des} = u_{pf}$;
8          $\psi_{des} = \psi_{pf}$;
9   mode = path_following;
10   **else**
11   **if** *last_mode is path_following* **then**
12   choose λ in accordance with COLREGs
13   **end**
14          $u_{des} = u_{oa}$;
15          $\psi_{des} = \psi_{oa}(\lambda)$;
16   mode = obstacle_avoidance;
17   **end**
18   last_mode = mode
19 **end**

Algorithm 1: Set-based guidance algorithm.

E. Surge and Yaw Controllers

This section presents surge and yaw controllers to ensure tracking of the desired surge velocity $u_{des}(t)$ and heading $\psi_{des}(t)$ provided by the set-based guidance system presented in the previous subsection. A feedback linearizing P-controller is used to ensure tracking of the desired relative

Input: σ, $\dot{\sigma}$, $\sigma_{\min}$, $\sigma_{\max}$

1 **if** $\sigma_{\min} < \sigma < \sigma_{\max}$ **then**
2 | **return** True;
3 **else if** $\sigma \leq \sigma_{\min}$ *and* $\dot{\sigma} \geq 0$ **then**
4 | **return** True;
5 **else if** $\sigma \leq \sigma_{\min}$ *and* $\dot{\sigma} < 0$ **then**
6 | **return** False;
7 **else if** $\sigma \geq \sigma_{\max}$ *and* $\dot{\sigma} \leq 0$ **then**
8 | **return** True;
9 **else**
10 | **return** False;
11 **end**

Algorithm 2: The boolean function in_T_C.

surge velocity $u_{\text{des}}(t)$:
$$\tau_u = -F_u(v,r) + \frac{d_{11}}{m_{11}} u_{\text{des}} + \dot{u}_{\text{des}} - k_u(u - u_{\text{des}}) \qquad (30)$$
The gain $k_u > 0$ is constant. Part of the damping is not canceled in order to guarantee some robustness with respect to model uncertainties. Similarly, a feedback linearizing PD-controller is used to track the desired yaw angle ψ_{des}. In this case $\dot{\psi}_{\text{des}}(t)$ is calculated by taking the time derivative of $\psi_{\text{des}}(t)$. Note that to prevent $\dot{\psi}_{\text{des}}$ growing very large when switching between path following and collision avoidance, a smoothing function may be applied (see Section VI).
$$\tau_r = -F_r(u,v,r) + \ddot{\psi}_{\text{des}} - k_\psi(\psi - \psi_{\text{des}}) - k_r(\dot{\psi} - \dot{\psi}_{\text{des}}), \qquad (31)$$
where k_ψ and k_r are strictly positive constant controller gains.

V. MAIN RESULT

This section presents the conditions under which the proposed control system achieves the control objectives (5)-(7).

Theorem 2. *Given an underactuated USV described by the dynamical system (4). If Assumptions 1-8 hold, and the surge and yaw references provided by the set-based guidance system in Algorithm 1 are tracked, the control objective (5) is satisfied. Furthermore, as long as the system is in path following mode, the control objective (6) is also fulfilled.*

Proof. In collision avoidance mode, the guidance laws for surge and yaw (15) ensure that the distance between the USV and an obstacle at position $\boldsymbol{p}_{\text{o}}(t)$, denoted ρ, converges to a constant value R_{o} (Theorem 1). If Assumption 8 is satisfied, this mode is always activated at a distance large enough that $\rho \to R_{\text{o}}$ without overshoot. Hence, we can apply the proof in [18] regarding satisfaction of set-based tasks with a valid set defined in (29). Thus, the first control objective is satisfied. Furthermore, the control objective (6) is fulfilled in path following mode by Assumption 5. $\qquad \square$

Proposition 1. *Given an underactuated USV described by the dynamical system (4). If Assumptions 1-8 hold, the controllers (30) and (31) ensure that the references provided by the set-based guidance system in Algorithm 1 are tracked, and the control objective (7) is satisfied.*

Proof. See Appendix C. $\qquad \square$

VI. SIMULATION: STRAIGHT LINE PATH

This section presents simulation results in the case where the desired path C is a straight line path, and where a traditional LOS guidance law is used for path following. Without loss of generality, we assume that the inertial frame has been rotated so the path is aligned with the inertial x-axis. Thus, the cross-track error of the path is given by the vehicle y-position and the LOS guidance law for path following is
$$\psi_{\text{pf}} = \arctan\left(-\frac{y}{\Delta}\right). \qquad (32)$$
In the simulations, we use the vehicle model described by (4) with numeric values given in [22]. The desired surge velocity is chosen to be 4 m/s both during path following and obstacle avoidance, i.e. $u_{\text{pf}} = u_{\text{oa}} = 4$ m/s. The look-ahead distance Δ is chosen as $\Delta = 75$ m, which is in accordance with the condition given in [22] for stability of the path following guidance control system. Furthermore, the controller gains are chosen as $k_u = 0.1$ s^{-1}, $k_\psi = 0.04$ s^{-2} and $k_r = 0.9$ s^{-1}. Three obstacles moving at constant speed have been added to the simulation, see Table I. Furthermore, a smoothing function has been implemented to prevent jumps in the desired heading when switching between path following and collision avoidance. Note that this smoothing function ensures a smooth transition over time between ψ_{pf} and ψ_{oa} when switching between modes, but is not active in deciding whether or not a switch in the set-based guidance occurs. Hence, it does not suffer from the same drawbacks as the potential field approach. The implemented smoothing function has been chosen as
$$\alpha(t, t_{\text{switch}}) = (1/\pi)\arctan(5(t - t_{\text{switch}} - 2)) + (1/2). \qquad (33)$$
To test robustness, these simulations consider only obstacles that do not abide by COLREGs, meaning that they do nothing to prevent a collision with the USV.

Obstacle	Details
Obstacle 1	• $R_{\text{o}} = 75$ m • $R_{\text{m}} = 220$ m • Initial position: $\boldsymbol{p}_{\text{o}}(0) = [300, 25]^T$ m • Velocity: $\dot{\boldsymbol{p}}_{\text{c}}(t)) = [-0.3, 0.0]^T$ m/s
Obstacle 2	• $R_{\text{o}} = 100$ m • $R_{\text{m}} = 250$ m • Initial position: $\boldsymbol{p}_{\text{o}}(0) = [780, 125]^T$ m • Velocity: $\dot{\boldsymbol{p}}_{\text{c}}(t)) = [0.0, -0.5]^T$ m/s
Obstacle 3	• $R_{\text{o}} = 100$ m • $R_{\text{m}} = 200$ m • Initial position: $\boldsymbol{p}_{\text{o}}(0) = [960, 50]^T$ m • Velocity: $\dot{\boldsymbol{p}}_{\text{c}}(t)) = [1, 0]^T$ m/s

TABLE I: Table of implemented obstacles in simulation.

The simulation results are illustrated in Fig 5. The vessel successfully avoids the obstacles (Fig. 6) and converges to the desired straight line path when it is possible to do so. Figure 7 illustrates the path following cross-track error, which converges to zero in path following mode, and the desired and actual surge velocity and heading. The controllers (30) and (31) are able to track their references well. Thus, the control objectives (5)-(7) are satisfied.

VII. CONCLUSIONS

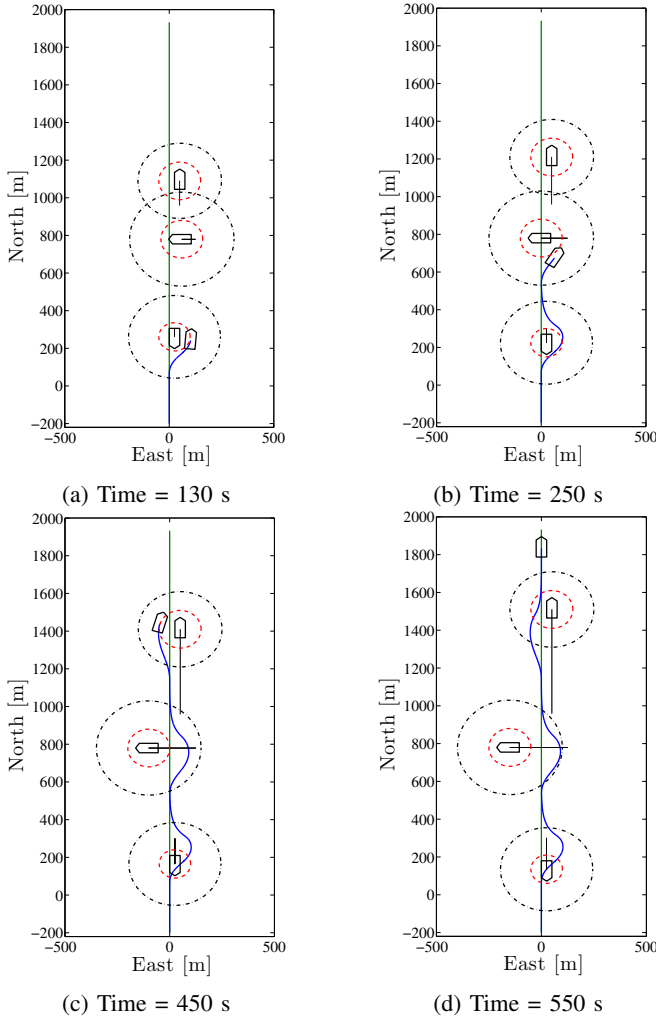This paper has presented a guidance and control system for an USV that allows for collision avoidance of moving

(a) Time = 130 s

(b) Time = 250 s

(c) Time = 450 s

(d) Time = 550 s

Fig. 5: Trajectory for straight line path following with collision avoidance. Desired path in green, USV path in blue and the radii R_o and R_m of the obstacles in dashed red and black, respectively. In this simulation, the USV encounters three obstacles corresponding to a head-on, crossing from right and overtaking situation. All obstacles are successfully circumvented in a COLREGs manner and the USV converges back to the path as soon as this is safe.

obstacles while following a predefined desired path. Based on recent results in set-based guidance theory, this paper develops a collision avoidance method that take the underactuation of the USV into account. The proposed system switches between two guidance laws that, if satisfied, ensure path following and collision avoidance, respectively. Note that this approach can be used with any combination of methods for path following and collision avoidance.

Furthermore, this paper has suggested a specific guidance law for the collision avoidance mode that will, if satisfied, make the USV track a circle with a constant safe radius about the moving obstacle center. The suggested guidance law for collision avoidance has a parameter $\lambda = \pm 1$ corresponding to clockwise and counterclockwise motion. A method for
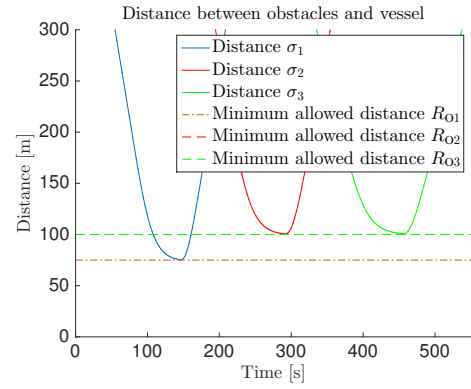

Fig. 6: Distance between the USV and the three obstacles over time. The distance is always greater or equal to the minimum allowed safe distance R_o, confirming that control objective 1 is satisfied.

choosing λ has been presented to ensure that the USV abides by COLREGs while avoiding the obstacles.

The set-based guidance system has been proved to prevent collisions given that certain, specified assumptions on the obstacle velocity are satisfies and the references provided by the guidance system are tracked. Furthermore, the proposed controllers ensure exponential tracking of the references.

Presented simulation results illustrate the effectiveness of the proposed method. To prove robustness, the simulated obstacles do not abide by COLREGs, and the USV still successfully circumvents them in a COLREGs manner and converges back to the desired path as soon as this is safe.

Future work includes expanding the results to the case of overlapping obstacles and experimental verification.

APPENDIX A - VESSEL MODEL FUNCTIONS

$$F_u(v,r) = \frac{m_{22}v + m_{23}r}{m_{11}}r \tag{34}$$

$$X(u) = \frac{m_{23}^2 - m_{11}m_{33}}{m_{22}m_{33} - m_{23}^2}u + \frac{d_{33}m_{23} - d_{23}m_{33}}{m_{22}m_{33} - m_{23}^2} \tag{35}$$

$$Y(u) = \frac{m_{22}m_{23} - m_{11}m_{23}}{m_{22}m_{33} - m_{23}^2}u - \frac{d_{22}m_{33} - d_{32}m_{23}}{m_{22}m_{33} - m_{23}^2} \tag{36}$$

$$F_r(u,v,r) = \frac{m_{23}d_{22} - m_{22}(d_{32} + (m_{22} - m_{11})u)}{m_{22}m_{33} - m_{23}^2}v$$
$$+ \frac{m_{23}(d_{23} + m_{11}u) - m_{22}(d_{33} + m_{23}u)}{m_{22}m_{33} - m_{23}^2}r \tag{37}$$

APPENDIX B - PROOF OF THEOREM 1

The error dynamics is given by

$$\dot{e} = \dot{R}_o - \dot{\rho} = -\dot{\rho}, \tag{38}$$

where $\dot{\rho}$ is defined in (27). Under the conditions of Theorem 1, $u = u_{oa}$ (14) and $\psi = \psi_{oa}$ (15). It can be shown that this reduces the error dynamics to

$$\dot{e} = -\frac{U_{oa}}{\sqrt{\Delta^2 + (e+k)^2}}e - \frac{U_{oa}}{\sqrt{\Delta^2 + (e+k)^2}}k + V_o \tag{39}$$

Furthermore, given the proposed solution of k (17)-(18),

$$-\frac{U_{oa}}{\sqrt{\Delta^2 + (e+k)^2}}k + V_o \equiv 0,$$

so

$$\dot{e} = -\frac{U_{oa}}{\sqrt{\Delta^2 + (e+k)^2}}e \tag{40}$$

Using the positive definite Lyapunov function $V(e) = 0.5e^2$,

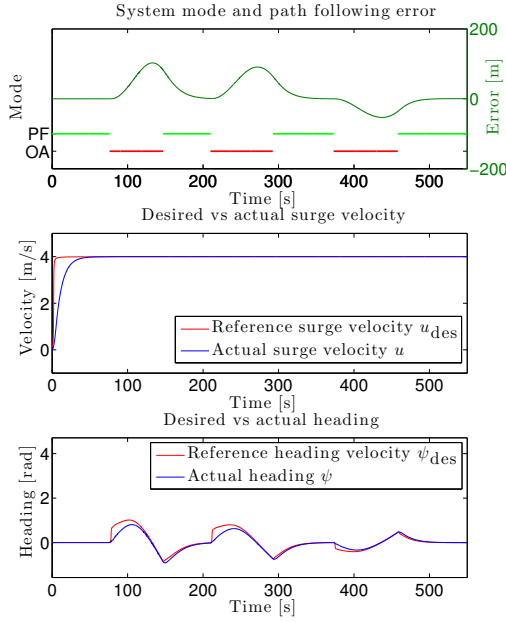$$\dot{V} = -\frac{U_{oa}}{\sqrt{\Delta^2 + (e+k)^2}}e^2 \tag{41}$$

Fig. 7: The path following error over time (top) and the reference vs. actual surge velocity (center) and heading (bottom). The UVS follows the path as long as this is possible without colliding and deviates from it when it is necessary to avoid obstacles. When the system returns to path following mode the USV converges back to the desired path. The controllers are able to track the references for u and ψ.

is negative definite and hence the equilibrium point $e = 0$ of (39) is UGAS [24].

APPENDIX C - PROOF OF PROPOSITION 1

We define the following error signals:

$$\tilde{u} = u - u_{\mathrm{des}}, \quad \tilde{\psi} = \psi - \psi_{\mathrm{des}}, \quad \tilde{r} = r - \dot{\psi}_{\mathrm{des}}$$

The surge and yaw controllers (30) and (31) reduce the error dynamics to

$$\dot{\boldsymbol{\xi}} = \begin{bmatrix} \dot{\tilde{u}}_r \\ \dot{\tilde{\psi}} \\ \ddot{\tilde{\psi}} \end{bmatrix} = \begin{bmatrix} -(k_{u_r} + \frac{d_{11}}{m_{11}}) & 0 & 0 \\ 0 & 0 & 1 \\ 0 & -k_\psi & -k_r \end{bmatrix} \begin{bmatrix} \tilde{u}_r \\ \tilde{\psi} \\ \dot{\tilde{\psi}} \end{bmatrix} = \boldsymbol{\Lambda} \boldsymbol{\xi} \quad (42)$$

The system is linear and time-invariant. All controller gains and d_{11}/m_{11} are strictly positive, meaning that $\boldsymbol{\Lambda}$ is Hurwitz and the origin $\boldsymbol{\xi} = 0$ is UGES. Thus the error signals converge to zero and the control objective (7) is satisfied.

ACKNOWLEDGMENTS

REFERENCES

[1] T. I. Fossen, *Handbook of Marine Craft Hydrodynamics and Motion Control*. Wiley, 2011.

[2] T. I. Fossen, M. Breivik, and R. Skjetne, "Line-of-sight path following of underactuated marine craft," *Proc. 6th IFAC Conference on Manoeuvering and Control of Marine Craft*, pp. 244–249, 2003.

[3] S. Oh and J. Sun, "Path following of underactuated marine surface vessels using line-of-sight based model predictive control $," *Ocean Engineering*, vol. 37, no. 2-3, pp. 289–295, 2010.

[4] R. Skjetne, U. Jorgensen, and A. R. Teel, "Line-of-sight path-following along regularly parametrized curves solved as a generic maneuvering problem," in *Proc. IEEE Conference on Decision and Control and European Control Conference*, 2011, pp. 2467–2474.

[5] E. Borhaug and K. Y. Pettersen, "LOS path following for underactuated underwater vehicle," in *Proc. 7th IFAC Conference on Manoeuvring and Control of Marine Craft*, 2006.

[6] W. Caharija, M. Candeloro, K. Y. Pettersen, and A. J. Sorensen, "Relative Velocity Control and Integral LOS for Path Following of Underactuated Surface Vessels," *Proc. 9th IFAC Conference on Manoeuvring and Control of Marine Craft*, pp. 380–385, Sept. 2012.

[7] S. Moe, W. Caharija, K. Y. Pettersen, and I. Schjolberg, "Path following of underactuated marine surface vessels in the presence of unknown ocean currents," in *Proc. American Control Conference*, Portland, OR, USA, 2014, pp. 3856–3861.

[8] A. P. Aguiar and J. P. Hespanha, "Trajectory-Tracking and Path-Following of Underactuated Autonomous Vehicles With Parametric Modeling Uncertainty," *IEEE Transactions on Automatic Control*, vol. 52, no. 8, pp. 1362–1379, 2007.

[9] K. D. Do, J. Pan, and Z. P. Jiang, "Robust and adaptive path following for underactuated autonomous underwater vehicles," vol. 31, no. 16, pp. 1967–1997, 2004.

[10] P. Encarnacao and A. Pascoal, "Combined trajectory tracking and path following: an application to the coordinated control of autonomous marine craft," in *Proc. 40th IEEE Conference on Decision and Control*, vol. 1, 2001, pp. 964–969.

[11] Y. Kuwata, M. T. Wolf, D. Zarzhitsky, and T. L. Huntsberger, "Safe Maritime Autonomous Navigation With COLREGS , Using Velocity Obstacles," *IEEE Journal of Oceanic Engineering*, vol. 39, no. 1, pp. 110–119, 2014.

[12] O. Khatib, "Real-time obstacle avoidance for manipulators and mobile robots," in *Proc. IEEE International Conference on Robotics and Automation*, vol. 2, 1985, pp. 500–505.

[13] D. Fox, W. Burgard, and S. Thrun, "The dynamic window approach to collision avoidance," *Robotics Automation Magazine, IEEE*, vol. 4, no. 1, pp. 23–33, Mar. 1997.

[14] Ø. A. G. Loe, *Collision Avoidance for Unmanned Surface Vehicles*. Master's Thesis, Norwegian University of Science and Technolody, 2008.

[15] J. van den Berg, S. J. Guy, M. Lin, and D. Manocha, "Reciprocal n-Body Collision Avoidance," in *International Symposium on Robotics Research*, 2011, pp. 3–19.

[16] Y. Koren and J. Borenstein, "Potential field methods and their inherent limitations for mobile robot navigation," in *Proc. IEEE International Conference on Robotics and Automation*, no. April, 1991, pp. 1398–1404.

[17] G. Antonelli, S. Moe, and K. Y. Pettersen, "Incorporating Set-based Control within the Singularity-robust Multiple Task-priority Inverse Kinematics," in *Proc. 23rd Mediterranean Conference on Control and Automation*, 2015.

[18] S. Moe, A. R. Teel, G. Antonelli, and K. Y. Pettersen, "Stability Analysis for Set-based Control within the Singularity-robust Multiple Task-priority Inverse Kinematics Framework," in *Proc. 54th IEEE Conference on Decision and Control*, Osaka, Japan, 2015.

[19] S. Moe, G. Antonelli, K. Y. Pettersen, and J. Schrimpf, "Experimental Results for Set-based Control within the Singularity-robust Multiple Task-priority Inverse Kinematics Framework," in *Proc. IEEE International Conference on Robotics and Biomimetics*, 2015.

[20] E. Zereik, A. Sorbara, M. Bibuli, G. Bruzzone, and M. Caccia, "Priority Task Approach for USVs ' Path Following Missions with Obstacle Avoidance and Speed Regulation," in *Proc. 10th Conference of Manoeuvering and Control of Marine Craft*, 2015.

[21] E. Borhaug, A. Pavlov, and K. Y. Pettersen, "Integral LOS control for path following of underactuated marine surface vessels in the presence of constant ocean currents," in *Proc. 47th IEEE Conference on Decision and Control*, 2008, pp. 4984–4991.

[22] E. Fredriksen and K. Y. Pettersen, "Global κ-exponential way-point manoeuvering of ships," in *Proc. 43rd IEEE Conference on Decicion and Control*, 2004, pp. 5360–5367.

[23] M. R. Benjamin, J. J. Leonard, C. J. A., and P. M. Newman, "A method for protocol-based collision avoidance between autonomous marine surface craft," *Journal of Field Robotics*, vol. 23, no. 5, 2006.

[24] H. K. Khalil, *Nonlinear systems*. Prentice Hall PTR, 2002.